

## String method for the study of rare events

Weinan E,<sup>1</sup> Weiqing Ren,<sup>2</sup> and Eric Vanden-Eijnden<sup>2</sup>

<sup>1</sup>*Department of Mathematics and PACM, Princeton University, Princeton, New Jersey 08544*

<sup>2</sup>*Courant Institute, New York University, New York, New York 10012*

(Received 7 January 2002; published 12 August 2002)

We present an efficient method for computing the transition pathways, free energy barriers, and transition rates in complex systems with relatively smooth energy landscapes. The method proceeds by evolving strings, i.e., smooth curves with intrinsic parametrization whose dynamics takes them to the most probable transition path between two metastable regions in configuration space. Free energy barriers and transition rates can then be determined by a standard umbrella sampling around the string. Applications to Lennard-Jones cluster rearrangement and thermally induced switching of a magnetic film are presented.

DOI: 10.1103/PhysRevB.66.052301

PACS number(s): 82.20.Wt, 02.70.-c, 05.10.-a

The dynamics of complex systems is often driven by rare but important events (for a review see, e.g., Ref. 1). Well-known examples include nucleation events during phase transitions, conformational changes in macromolecules, and chemical reactions. The long time scale associated with these rare events is a consequence of the disparity between the effective thermal energy and typical energy barrier of the systems. The dynamics proceeds by long waiting periods around metastable states followed by sudden jumps from one state to another.

Sophisticated numerical techniques have been developed to find the transition pathways and transition rates between metastable states in complex systems for which the mechanism of transition is not known beforehand.<sup>2-4</sup> With the exception of the transition path sampling technique,<sup>3</sup> most of these methods seem to require that the energy landscape be relatively smooth. One typical example of such techniques is the nudged elastic band (NEB) method.<sup>4</sup> The NEB method connects the initial and final states by a chain of states. The states move in a force field which is a combination of the normal component of the potential force and the tangential component of the spring force connecting the states. The spring force helps to evenly space the states along the chain.

In this paper we propose an alternative approach for computing transition pathways, free energy barriers, and transition rates. We sample the configuration space with strings, i.e., smooth curves with intrinsic parametrization such as arc length or energy-weighted arc length which connect two metastable states (or regions)  $A$  and  $B$ . The string satisfies a differential equation which by construction guarantees that it evolves to the most probable transition pathway connecting  $A$  and  $B$ . One can then perform an umbrella sampling of the equilibrium distribution of the system in the hyperplanes normal to the string and thereby determine free energy barriers and transition rates.

Consider the example of a system modeled by

$$\gamma \dot{q} = -\nabla V(q) + \xi(t), \quad (1)$$

where  $\gamma$  is the friction coefficient and  $\xi(t)$  is a white noise with  $\langle \xi_j(t) \xi_k(0) \rangle = 2\gamma k_B T \delta_{jk} \delta(t)$ . The metastable states are localized around the minima of the potential  $V(q)$ . Assuming  $V(q)$  has at least two minima  $A$  and  $B$ , we look for the

minimal energy paths (MEP's) connecting these states. By definition, a MEP is a smooth curve  $\varphi^*$  connecting  $A$  and  $B$  which satisfies

$$(\nabla V)^\perp(\varphi^*) = 0, \quad (2)$$

where  $(\nabla V)^\perp$  is the component of  $\nabla V$  normal to  $\varphi^*$ . The MEP's are the most probable transition pathways for Eq. (1) since with exponentially high probability it is by these paths that the system switches back and forth between states  $A$  and  $B$  under the action of a small thermal noise.<sup>5</sup> It is interesting to note that the solutions of Eq. (2) also provide relevant information about the Langevin equation:

$$\dot{q} = p, \quad \dot{p} = -\nabla V(q) - \gamma p + \xi(t). \quad (3)$$

Indeed, the metastable regions for Eqs. (1) and (3) coincide, and the transition pathways for Eqs. (3) can be easily determined from the transition pathways for Eq. (1) because they traverse the same sequence of critical points. As a result the transition rates for Eqs. (3) for an arbitrary friction coefficient  $\gamma$  can be obtained by considering the high friction evolution equation (1)—see Eq. (10) below.

Let  $\varphi$  be a string (but not necessarily a MEP) connecting  $A$  and  $B$ . A simple method to find the MEP is to evolve  $\varphi$  according to

$$u^\perp = -(\nabla V)^\perp(\varphi), \quad (4)$$

where  $u^\perp$  denotes the normal velocity of  $\varphi$ , since stationary solutions of Eq. (4) satisfy Eq. (2). For numerical purposes it is convenient to have a parametrized version of Eq. (4), keeping in mind, however, that the parametrization can be arbitrarily chosen since both Eqs. (2) and (4) are intrinsic. Denote by  $\varphi(\alpha, t)$  the instantaneous position of the string, where  $\alpha$  is some suitable parametrization. Then we can rewrite Eq. (4) as

$$\varphi_t = -[\nabla V(\varphi)]^\perp + r \hat{t}, \quad (5)$$

where for convenience we renormalized time  $t/\gamma \rightarrow t$ ,  $(\nabla V)^\perp = \nabla V - (\nabla V \cdot \hat{t}) \hat{t}$ , and  $\hat{t}$  is the unit tangent vector along  $\varphi$ ,  $\hat{t} = \varphi_\alpha / |\varphi_\alpha|$ . The scalar field  $r = r(\alpha, t)$  is a

Lagrange multiplier uniquely determined by the choice of parametrization. The simplest example is to parametrize  $\varphi$  by arc length normalized so that  $\alpha=0$  at  $A$ ,  $\alpha=1$  at  $B$ . Then Eq. (5) must be supplemented by the constraint

$$(|\varphi_\alpha|)_\alpha=0 \quad (6)$$

which determines  $r$ .<sup>6</sup> Other parametrizations can be straightforwardly implemented by modifying the constraint (6). For instance, a parametrization by energy-weighted arc length which increases the resolution at the transition states is achieved using the constraint  $[f(V(\varphi))|\varphi_\alpha|]_\alpha=0$ , where  $f(z)$  is some suitable monitor function satisfying  $f'(z)<0$ . In addition, the end points of the string need not be fixed and other boundary conditions can be used.

Because of the intrinsic description of the string, it is very simple to implement an efficient algorithm which solves Eq. (5) using a time-splitting scheme. The string is discretized into a number of points which move according to the first term  $-\nabla V(\varphi)^\perp$  at the right-hand side of Eq. (5). After a number of steps depending on the accuracy for the constraint (6), a reparametrization step is applied to reinforce Eq. (6). This costs  $O(N)$  operations where  $N$  is the number of discretization points along the string. At the reparametrization step it is also convenient to change  $N$  according to the accuracy requirement for the representation of the string.

The method certainly bears some similarities with the NEB method since one can think of the introduction of the spring force in the NEB method as a way of ensuring equal-distance parametrization by a penalty method—the NEB method gives an evolution equation which, in the continuum limit, is similar to Eq. (5) but with  $r$  given by  $r=\kappa\varphi_{\alpha\alpha}\cdot\hat{t}$  where  $\kappa$  is the artificial spring constant. As in other penalty methods, this numerical procedure introduces stiffness into the problem if the penalization parameter, here the elastic constant  $\kappa$ , is large and this limits the size of the time step. By using an intrinsic description, we eliminate this problem and speed up convergence. Furthermore, we gain the ability of using other parametrizations in a simple and flexible way. Finally, there is no simple way to change the number of discretization points along the chain in the NEB method.

It is natural to ask how the string method compares to the NEB method in terms of performance. However, an objective comparison does not seem straightforward since there are several different angles, such as the accuracy dependence on the number of discretization points and rate of convergence, which have to be examined. We therefore postpone this discussion to Ref. 8.

As a first example we look at the dynamics of seven atoms interacting via the Lennard-Jones potential on the plane. This example has been studied in detail in Ref. 7. In equilibrium the seven atoms form a hexagon. We are interested in the process in which the atom at the center migrates to an external position. The MEP's are not unique for this problem. One example of an MEP obtained via the string method is shown in Fig. 1; the critical points along this path coincide with the ones obtained in Ref. 7 by transition path sampling.

The string equation (5) essentially amounts to finding the MEP's by the method of steepest descent except that we are

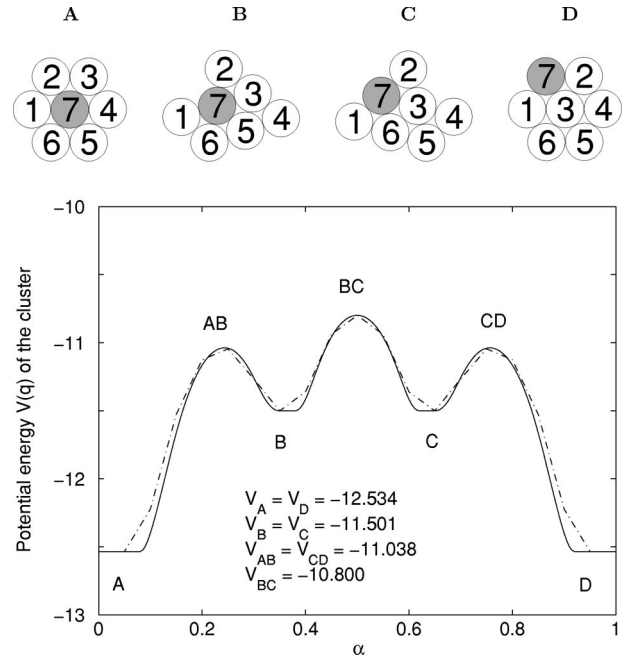


FIG. 1. Top figure: a transition pathway by which the central atom migrates to the surface in a seven-atom hexagonal Lennard-Jones cluster in the plane. The pictures show successive configurations corresponding to local minima of the potential energy along the path. Bottom figure: the potential energy along the path in natural units. The solid line corresponds to a simulation with  $N=200$  discretization points along the string and the dashed line  $N=20$ .

not working with any explicit object function to minimize. We can use advanced numerical techniques for solving nonlinear equations<sup>9</sup> to accelerate convergence to the MEP. We have developed a limited memory version of Broyden's method where Eq. (5) is replaced by

$$\varphi_t = -G^\perp[\nabla V(\varphi)]^\perp + r\hat{t}. \quad (7)$$

Here  $G^\perp$  is a matrix determined on the fly during the computations to approximate the inverse of the Hessian in the perpendicular hyperplane; the approximation is based on the past history of  $\varphi$  and does not require one to actually compute the Hessian (for details, see Ref. 8). In Fig. 2, we compare the convergence history of the steepest descent method and the Broyden-accelerated method applied to the seven-atom cluster problem. The Broyden-accelerated method converges much faster.

Once the MEP  $\varphi^*(\alpha)$  has been determined using the Broyden-accelerated string method, free energy barriers and transition rates can be computed by standard umbrella sampling of the equilibrium distribution of the system in  $S^*(\alpha)$ , the hyperplane normal to  $\varphi^*(\alpha)$ . Consider first the free energy difference along the string defined as  $F(\alpha) - F(0) = -k_B T \ln[Z(\alpha)/Z(0)]$  where

$$Z(\alpha) = \int_{S^*(\alpha)} e^{-\beta V(q)} d\sigma \quad (8)$$

is the partition function and  $\beta=1/k_B T$ . Using the identity  $\int \partial \ln Z / \partial \alpha d\alpha = \ln Z(\alpha)$ , we obtain from Eq. (8)

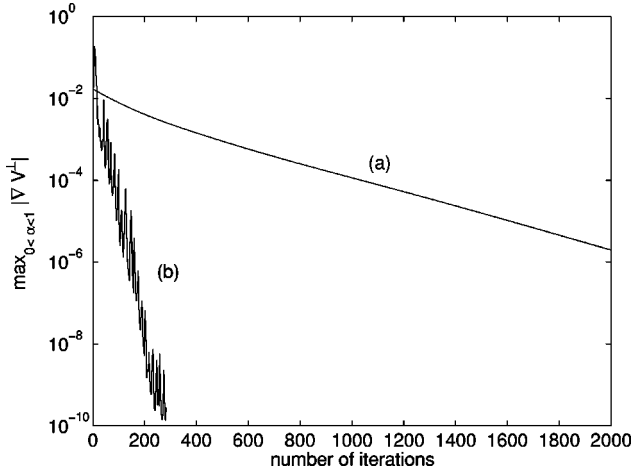


FIG. 2. The convergence history of the steepest descent method (a) and a limited memory version of Broyden's method (b) applied to the seven-atom cluster problem with  $N=200$  discretization points. We use  $\max_{0 \leq \alpha \leq 1} |(\nabla V)^\perp|$  to measure accuracy.

$$F(\alpha) - F(0) = \int_0^\alpha \langle (\hat{t}^* \cdot \nabla V) [(\hat{t}^* \cdot \varphi^*)_{\alpha'} - \hat{t}_\alpha^* \cdot q] \rangle d\alpha'. \quad (9)$$

Here  $\langle \cdot \rangle$  is the ensemble average with respect to the equilibrium distribution restricted in the hyperplane  $S(\alpha)$  and  $t^*$  is the unit tangent vector along  $\varphi^*$ . Equation (9) is similar to the standard thermodynamic integration<sup>10</sup> but is better suited for numerical purposes. In practice, we use ergodicity and replace the ensemble average in Eq. (9) by a time average over the solution of an equation similar to Eq. (1) but restricted in the hyperplane  $S(\alpha)$ . Following Kramers' original argument (see, e.g., Chap. 9 in Ref. 11), the transition rate can be expressed in terms of the free energy as

$$k_{A \rightarrow B} = \frac{2\sqrt{|\lambda_m|\lambda_s|}}{\pi(\gamma + \sqrt{\gamma^2 + 4|\lambda_s|})} e^{-\beta\Delta F}, \quad (10)$$

where  $\Delta F$  is free energy barrier along  $\varphi^*$ ,

$$\Delta F = \max_{0 \leq \alpha \leq 1} [F(\alpha) - F(0)], \quad (11)$$

and  $\lambda_m$  and  $\lambda_s$  are the (inverse square of) characteristic time scales at the minimum and maximum of the free energy

TABLE I. The rates for the various subprocesses in the transition shown in Fig. 1 in the seven-atom cluster problem. We use natural units and the same parameters as in Ref. 7 (for which, e.g.,  $k_B T / \Delta E_{A \rightarrow B} = 0.033$  and  $\gamma / 2\sqrt{|\lambda_s|} = 0.012$ —low friction limit). The rates  $k_{A \rightarrow B}$ ,  $k_{B \rightarrow A}$ , and  $k_{B \rightarrow C}$  correspond, respectively, to the rates for the subprocesses  $C_0^0 \rightarrow C_1^4$ ,  $C_1^4 \rightarrow C_0^0$ , and  $C_1^4 \rightarrow C_1^3$  identified in Ref. 7. The values labeled “string” were obtained by the noisy string method using Eqs. (9), (11), and (10). The values labeled “exact” were obtained using Eqs. (10) and (13), by identifying minima and saddle points along the transition path, computing the corresponding energy barrier  $\Delta E$ , and evaluating all the eigenvalues of the Hessian at the minima and the saddle points from the Hessian itself.

	$k_{A \rightarrow B} = k_{D \rightarrow C}$	$k_{B \rightarrow A} = k_{C \rightarrow D}$	$k_{B \rightarrow C} = k_{C \rightarrow B}$
String	$5.023 \times 10^{-13}$	$1.425 \times 10^{-4}$	$1.211 \times 10^{-6}$
Exact	$4.969 \times 10^{-13}$	$1.423 \times 10^{-4}$	$1.206 \times 10^{-6}$

along the transition path;  $\lambda_m$  and  $\lambda_s$  are given by  $|\varphi_\alpha|^{-2} F_{\alpha\alpha}$  evaluated at  $\alpha=0$  and  $\alpha=\alpha_s$ , respectively, where  $\alpha_s$  is the value at which the maximum in Eq. (11) is attained.<sup>12</sup>

The transition rates along the MEP obtained earlier for the seven-atom cluster were evaluated by the string method and are summarized in Table I.

The string method can easily be generalized to infinite-dimensional dynamical systems by introducing an appropriate norm in phase space. As an example, we consider the problem of thermally induced switching of a magnetic film. This problem is of great current interest in the magnetic recording industry.<sup>15</sup> (For an introduction to micromagnetism, see, e.g., Refs. 13,15; thermally induced switching is studied in Ref. 14). Landau-Lifshitz theory of micromagnetism provides an energy for a ferromagnetic sample  $\Omega$  which, after suitable nondimensionalization, reads

$$E[m] = A \int_\Omega |\nabla m|^2 d^3x + \int_\Omega \phi(m) d^3x + \int_{\mathbb{R}^3} |\nabla u|^2 d^3x, \quad (12)$$

where  $m$  is the magnetization distribution normalized so that  $|m|=1$ . The three terms represent, respectively, energies due to exchange, anisotropy, and stray field. The potential  $u$ , defined everywhere in space, solves  $\text{div}(-\nabla u + m) = 0$ , where  $m$  is extended as 0 outside  $\Omega$ .

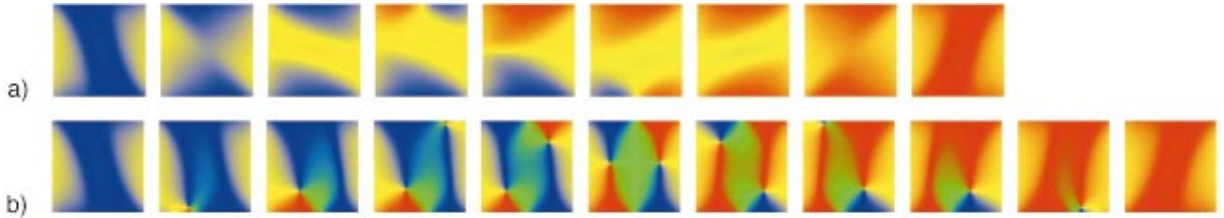


FIG. 3. (Color) Two of the paths (a) and (b) followed by the magnetization vector  $m$  during a switching. The pictures show the succession minimum-saddle-saddle-minimum. The out-of-plane component of  $m$  is very small (less than  $10^{-2}$ ) during the switching and we only plot its in-plane component with color coding: blue = right, red = left, yellow = up, green = down. For both paths, we used  $N=80$  discretization points along the string.

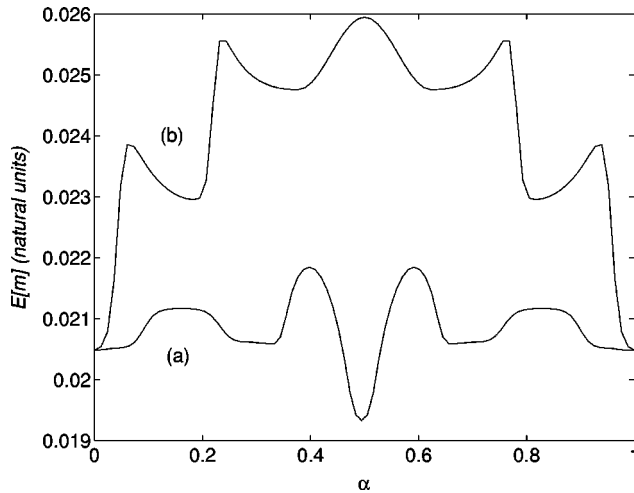


FIG. 4. The magnetic energy along the two paths (a) and (b) shown in Fig. 3.

Various switching pathways for Eq. (12) were obtained using the string method: two examples are shown in Fig. 3

and the energy along these paths is shown in Fig. 4. These paths illustrate two generic mechanisms for switching in magnetic films. Path (a), which is more favorable in thin samples, proceeds by domain wall motion, interior rotation, and switching of the edge domains. Path (b), which is more favorable for thicker films, proceeds by vortex nucleation, invasion of the sample, and vortex expulsion.

In conclusion, transition pathways and transition rates for complex systems with a relatively smooth energy landscape can be determined efficiently by evolving strings instead of points in configuration space. The intrinsic parametrization of the string leads to a simple and efficient algorithm for the numerical solution of its evolution equation and permits one to sample the configuration space in regions that otherwise would be practically inaccessible by standard Monte Carlo methods. In addition, our method does seem to have one distinct advantage over the NEB method; that is, it can be readily extended to situations when the energy landscape is rough (see Ref. 16).

We thank Roberto Car and Bob Kohn for helpful discussions. The work of W. E was supported in part by NSF Grant No. DMS01-30107.

<sup>1</sup>P. Hänggi, P. Talkner, and M. Borkovec, *Rev. Mod. Phys.* **62**, 251 (1990).

<sup>2</sup>I. V. Ionova and E. A. Carter, *J. Chem. Phys.* **98**, 6377 (1993); R. Olender and R. Elber, *ibid.* **105**, 9299 (1996); *J. Mol. Struct.: THEOCHEM* **398**, 63 (1997); A. Michalak and T. Ziegler, *J. Phys. Chem. A* **105**, 4333 (2001); D. Passerone and M. Parrinello, *Phys. Rev. Lett.* **87**, 108 302 (2001).

<sup>3</sup>C. Dellago, P. G. Bolhuis, F. S. Csajka, and D. Chandler, *J. Chem. Phys.* **108**, 1964 (1998).

<sup>4</sup>H. Jónsson, G. Mills, and K. W. Jacobsen, in *Classical and Quantum Dynamics in Condensed Phase Simulations*, edited by B. J. Berne *et al.* (World Scientific, Singapore, 1998); G. Henkelman and H. Jónsson, *J. Chem. Phys.* **113**, 9978 (2000).

<sup>5</sup>M. I. Freidlin and A. D. Wentzell, *Random Perturbations of Dynamical Systems*, 2nd ed. (Springer, New York, 1998).

<sup>6</sup>In this case  $r$  is given explicitly by

$$r = \alpha \int_0^1 \nabla V \cdot \hat{t}_{\alpha'} d\alpha' - \int_0^{\alpha} \nabla V \cdot \hat{t}_{\alpha'} d\alpha'$$

<sup>7</sup>C. Dellago, P. G. Bolhuis, and D. Chandler, *J. Chem. Phys.* **108**, 9236 (1998).

<sup>8</sup>W. E, W. Ren, and E. Vanden-Eijnden (unpublished).

<sup>9</sup>C. T. Kelley, *Iterative Methods for Linear and Nonlinear Equations* (SIAM, Philadelphia, 1995).

<sup>10</sup>D. Frenkel and B. Smit, *Understanding Molecular Simulations:*

*From Algorithms to Applications* (Academic Press, San Diego, 1996).

<sup>11</sup>C. W. Gardiner, *Handbook of Stochastic Methods*, 2nd ed. (Springer, New York, 1985).

<sup>12</sup>In the small temperature limit, the free energy difference can also be expressed as

$$\Delta F = \Delta E - k_B T \ln \sqrt{\frac{\det H_m^\perp}{\det H_s^\perp}}, \quad (13)$$

plus higher-order terms in  $k_B T$ , where  $\Delta E$  is the energy barrier along the MEP, and  $H_m^\perp$  and  $H_s^\perp$  are the Hessian matrices in the hyperplane perpendicular to the MEP evaluated at the minimum and the transition state (saddle), respectively. In the same limit  $\lambda_m$  and  $\lambda_s$  are the eigenvalues of the Hessian corresponding to the eigenvectors parallel to the MEP evaluated at the minimum and the transition state, respectively.

<sup>13</sup>A. Aharoni, *Introduction to the Theory of Ferromagnetism* (Oxford University Press, 1996).

<sup>14</sup>H.-B. Braun, *Phys. Rev. Lett.* **71**, 3557 (1993); *Phys. Rev. B* **50**, 16 485 (1994); **50**, 16 501 (1994); D. V. Berkov, *J. Magn. Magn. Mater.* **186**, 199 (1998); W. E, W. Ren, and E. Vanden-Eijnden (unpublished).

<sup>15</sup>R. P. Cowburn, *Philos. Trans. R. Soc. London, Ser. A* **358**, 281 (2000).

<sup>16</sup>W. E, W. Ren, and E. Vanden-Eijnden (unpublished).